Investigation of III-V GaP solar cell on silicon substrate

Soline Boyer-Richard, Fei Fan, Alexandre Beck, Christophe Levallois, Karine Tavernier, Tony Rohel, Rozenn Bernard, Antoine Létoublon, Charles Cornet, Olivier Durand

EPJ Photovoltaics **14**, 31 (2023)

https://doi.org/10.1051/epjpv/2023020

Available online at:
www.epj-pv.org

Special Issue on 'Recent Advances in Photovoltaics 2022', edited by Mohamed Amara, Thomas Fix, Jean-Paul Kleider, Judikaël Le Rouzo and Denis Mencaraglia

REGULAR ARTICLE OPEN ACCESS

Investigation of III-V GaP solar cell on silicon substrate

Soline Boyer-Richard*, Fei Fan, Alexandre Beck, Christophe Levallois, Karine Tavernier, Tony Rohel, Rozenn Bernard, Antoine Létoublon, Charles Cornet, and Olivier Durand

Université de Rennes, INSA Rennes, CNRS, Institut FOTON – UMR 6082, 35000 Rennes, France

Received: 3 March 2023 / Received in final form: 20 July 2023 / Accepted: 6 September 2023

Abstract. The best solar conversion efficiencies have been reached thanks to multijunction solar based on III-V semiconductors on GaAs or Ge substrates. While displaying high conversion efficiencies, these solar cells suffer from the high cost of such substrates. To benefit from both the low cost and technological maturity of silicon cells, III-V tandem cells on silicon seem a good compromise to overpass the theoretical efficiency limit of the Si single cells. To study the GaP/Si interface effect on the solar cell characteristic, a GaP n-i-p solar cell has been grown on silicon substrate. Two types of electrical contacts configurations have been processed: a top-top configuration in which the current does not see the GaP/Si interface and the top-bottom configuration where the electric current crosses the interface. A comparison of dark I-V, I-V under solar illumination, and EQE measurements on both configurations is performed. The top-bottom contacts configuration shows an EQE a little bit lower than the top-top contact one, likely due to lower carrier diffusion length or recombination at the lower interface. However, the result on the EQE of the top-bottom configuration is encouraging for the future development of the GaP-based/Si tandem solar cells, and any other tandem cell on silicon using GaP as an intermediate selective contact.

Keywords: Gallium phosphide / III-V on silicon / tandem cell

1 Introduction

Nowadays, the best solar conversion efficiencies have been reached thanks to multijunction solar cells consisting of a stacking of III-V semiconductor single junctions on GaAs or Ge substrates. While displaying high conversion efficiencies, these solar cells suffer from the high cost of such substrates. Therefore, a strategy is to develop a tandem cell on silicon, in order to benefit from both the low cost and technological maturity of silicon cells. Furthermore, this route surpasses the theoretical efficiency limit of the Si single cells. Indeed, theoretical studies have shown that a tandem cell consisting of a large bandgap material (ideally 1.6–1.7 eV) on a 1.1 eV Si cell would reach efficiencies above 40% [1–3]. Moreover, halide perovskites on silicon tandem cells have already reached 32.5% [4].

To obtain III-V tandem cells on silicon, several methods exist: wafer bonding, metamorphic growth and pseudomorphic growth. The main drawback of wafer bonding is the difference of expansion coefficients between III-V and silicon, which leads to the generation of cracks in solar cells. Metamorphic growth implies a large lattice mismatch, leading to dislocations in the solar cell which may be harmful for the carrier collection. Consequently, this strategy requires the use of dislocation localization such as the growth of a buffer with gradual composition prior to the growth of the absorber. Pseudomorphic approach satisfies both conditions of current matching and lattice matching between top cell and bottom cell. To this aim, we use GaP, grown by MBE, which is quasi lattice-matched with Si (0.4% of mismatch at 300K) and which displays a large bandgap of 2.3 eV. Due to its very high bandgap, GaP is not the ideal material to perform the top cell of a tandem cell. However, GaP-based diluted nitride solar cells on GaP substrate have already been studied to obtain top cells with a lower bandgap of 1.7 eV [5–7]. Towards the III-V solar cell on silicon using a GaP/Si interface, one also needs to know the influence of this interface. This is the aim of the present study.

A GaP n-i-p photodiode has been grown on silicon substrate. Two types of electrical contacts configurations have been studied: a top-top configuration in which the current does not see the GaP-Si interface in normal solar cell operation, and the top-bottom configuration where the electric current crosses the interface. A comparison of electrical characteristics on both configurations is reported to validate the use of the GaP/Si interface. We first detail

* e-mail: soline.boyer@insa-rennes.fr

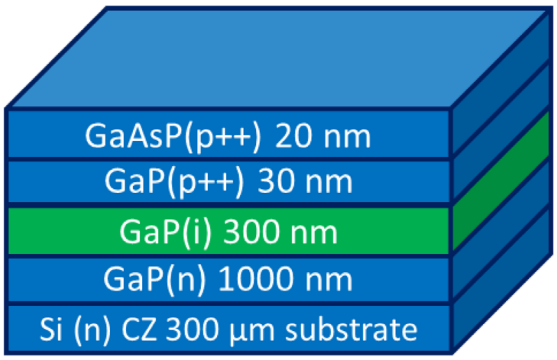

Fig. 1. Structure of the GaP-based n-i-p heterostructure on silicon.

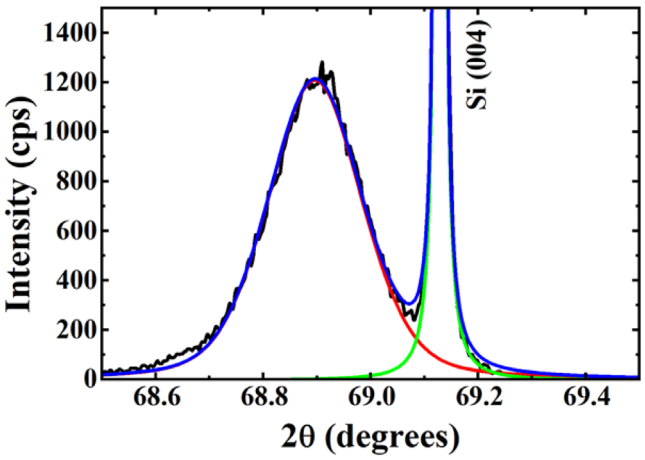

Fig. 2. θ/2θ XRD results of the GaP-based n-i-p heterostructure on Si around both the Si (004) and GaP (004) diffraction peaks, and including simulations of the GaP (004) peak (red solid line), the Si (004) peak (green solid line) using a pseudo-Voigt functions. The blue solid line represents the sum of both the simulations.

the technological steps used to process the two types of solar cells. I-V and EQE experimental results are presented and compared to quantify the effect of the GaP-Si interface on electrical characteristics.

2 Experimental

2.1 Sample epitaxial structure

The sample studied is a p-i-n photodiode grown onto 6°-off Si (001) substrate [8] with an absorber made with a simple 300 nm-thick GaP binary layer. Figure 1 shows the sample structure. The p-i-n junction is grown using solid source molecular beam epitaxy. First, a 1 µm-thick *n*-doped GaP buffer layer is grown (doping 8.10^{17} cm^{-3}) on a *n*-doped Si substrate. This large thickness of 1 µm has been grown to ensure a sufficient good crystallinity of the GaP absorber and to ensure a sufficient separation between the absorber and the GaP/Si interface. Then a 300 nm-thick undoped GaP absorber is surmounted by a 30 nm p++ GaP with a doping rate of 1.10^{19} cm^{-3}. Finally, a 20 nm p++ GaAsP (doping rate: 3.10^{19} cm^{-3}), with 20% of As, is deposited to ensure good electrical contact on top.

2.2 Structural characterization

To study the structural quality of the grown sample before technological processing, an analysis is performed by XRD measurement. From Figure 2 which shows the θ/2θ XRD result, we can clearly see that the GaP is fully relaxed. Indeed, since the critical thickness of GaP/Si is below 100 nm [7], and the thickness of our GaP stacking is more than 1 µm, it is expected to be fully relaxed [9]. A calculation of the diffraction correlation length along the growth direction, from the integral peak width (Fig. 2 right) and using the Scherrer's law, gives 42.5 nm, much less than the nominal layer thickness. Since this value is inversely proportional to the defect's density, this means that the layer contains a non-negligible density of crystalline defects, likely due to the relaxation processes. However, the absence of any other diffraction peaks than the (001) diffraction ones indicate a strong epitaxy of the GaP on silicon. Moreover, the pole figures performed on the thick GaP/Si (001) are characteristics of an epitaxy of the GaP onto the Si substrate, with micro twins' defects [10].

2.3 Technological process

After the crystal growth of p-i-n junctions, the technological steps consist of depositing the ohmic contacts and insulating each solar cell. Two types of architecture are developed (Fig. 3): 5.25×5.25 mm^2 cells with Busbar and fingers contacts on the front face and full-surface contacts on the back ("top-bottom"); and 365×290 µm^2 cells with both contacts on the front face ("top-top"). Figures 4 and 5 describe the technological process for each type of diode. The metal contacts are deposited on the cells in an electron beam evaporator under vacuum. The Ti/Pt/Au (p contact) [11] and Ni/Au/Ge (n contact) [5] sequences are deposited on the substrate after a deoxidation step in a 5% hydrofluoric acid solution. In the case of p contact (on the front side of the cell), the contact pattern is obtained by lift-off. Etching is essential for photovoltaics, because it makes it possible to isolate each cell in the form of a mesa and to avoid strong leakage current in reverse bias. Our large size cell is compatible with chemical solution etching techniques. We use a solution of $HCl:H_2O:H_2O_2 = 40:1:2$. Plasma etching is used to isolate the top-top cells. In the top-bottom configuration, ionic implantation of phosphorus has been performed to *n*-dope the silicon substrate after the MBE growth, and Al contact (Al with 1% Si) is used.

2.4 Quantum efficiency measurements

The EQE measurements were carried out with a Bentham PVE 300 apparatus. The generated electrical current is measured using a synchronous detection amplifier for each wavelength by a chopper. A silicon solar cell is included as a reference for calibrating the device before each measurement.

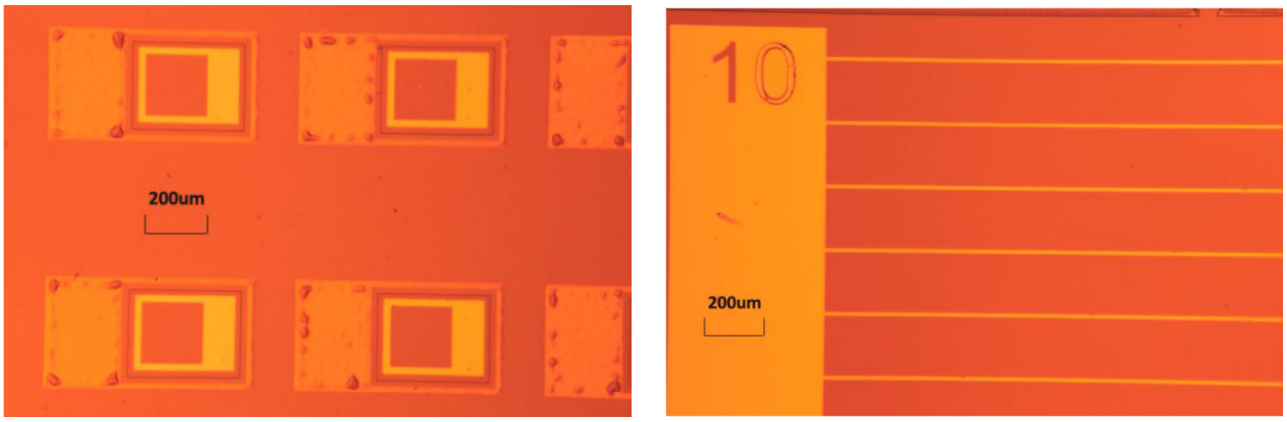

Fig. 3. Optical pictures of the two different solar cells architectures; top-top cell (left) and top-bottom cell (right).

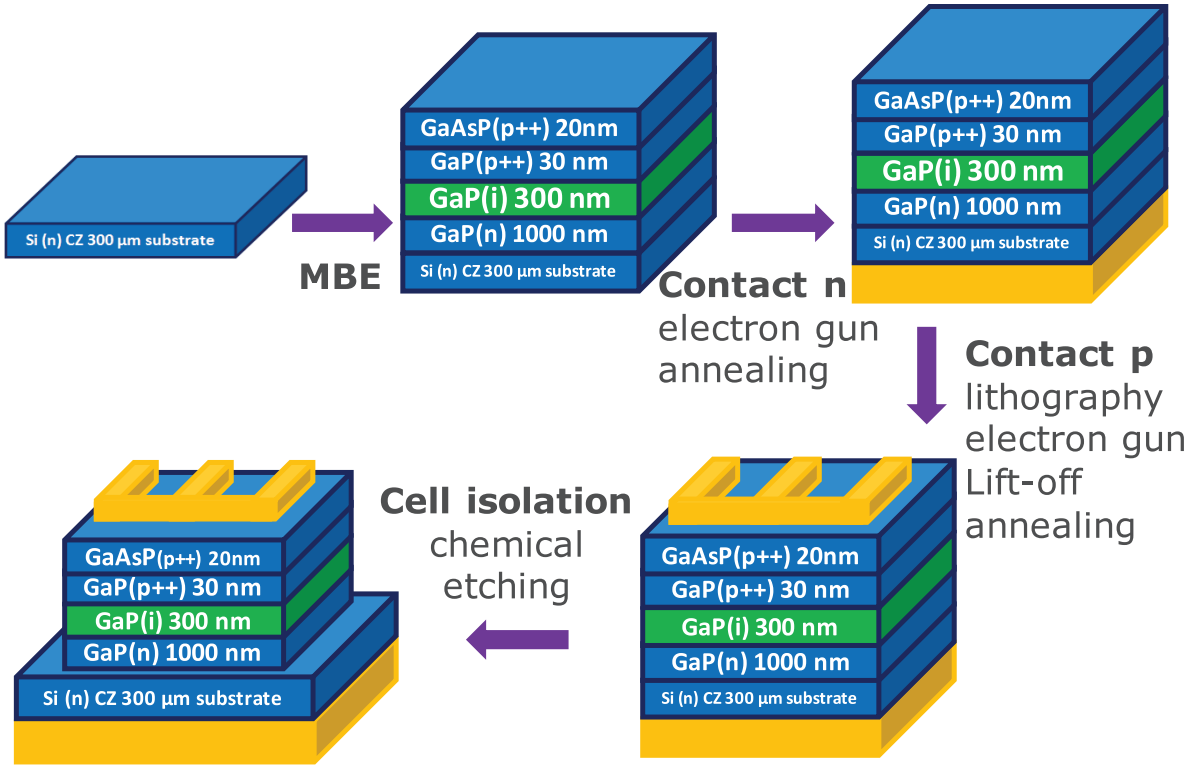

Fig. 4. Technological steps to manufacture the GaP-based cells in the case of "top-bottom" contacts.

3 Results and discussion

3.1 EQE measurements and absorption

The EQE measurements were performed to study the electro-optical properties of the GaP solar cells with the top-top contacts compared to the top-bottom contacts. The surface area of the light spot used during the EQE measurement is 740 µm × 740 µm. The surface area of the top-top sample is 200 µm × 195 µm which is much smaller than the light spot. In this situation, the EQE result are corrected by a coefficient equal to 14, corresponding to the surface ratio between the light spot area and the sample window area. Due to the small size of the sample window area, EQE results are slightly noisy. To obtain more accurate results for such small diodes, EQE result for top-top cells is an average between results obtained on 4 different samples which present almost the same characteristics. On the contrary, the surface area of the top-bottom sample is: 0.525 cm × 0.525 cm which is much larger than the light spot. In this situation, there is no need to correct the EQE result for the top-bottom sample and the curve presented is obtained with one specific sample. EQE results are presented on Figure 6. Figure 7 presents Tauc plots, used to determine the absorption thresholds from EQE [12,13]. From the top-top measurements (upper Fig. 7), only the direct bandgap

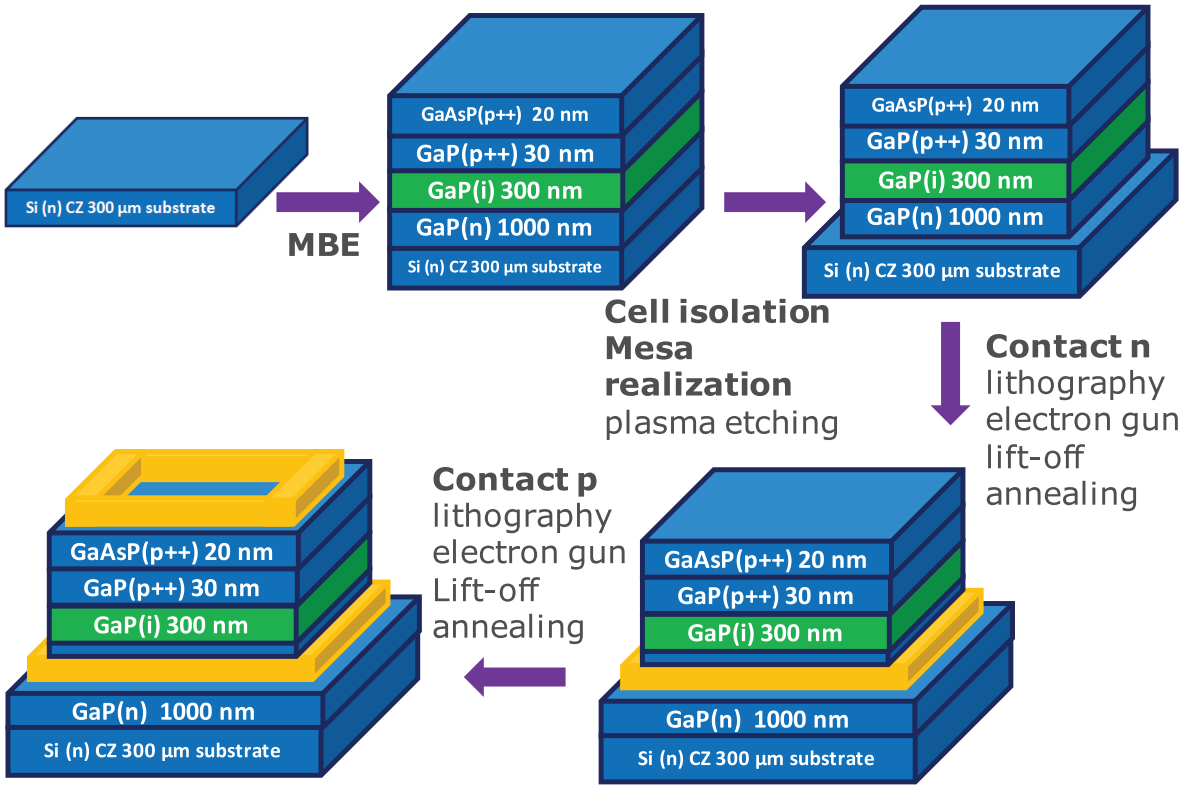

Fig. 5. Technological steps to manufacture the GaP-based cells in the case of "top-top" contacts.

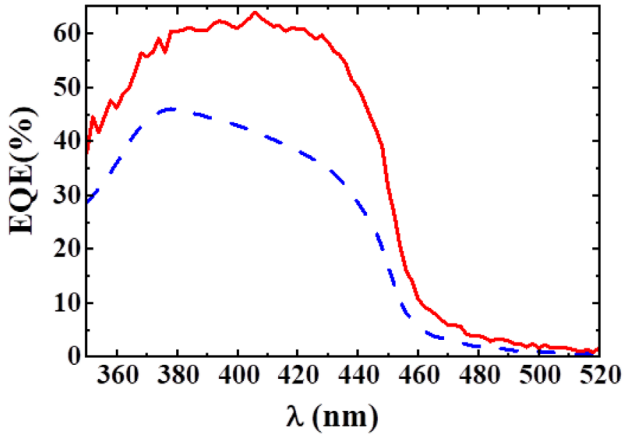

Fig. 6. External quantum efficiency (EQE) curve from the p-i-n GaP solar cell in both the top-top electrical contacts configuration (solid red line) and the top-bottom electrical contacts configuration (blue dashed line).

absorption threshold is measured equal to 2.73 eV. The indirect bandgap cannot be measured, because the uncorrected red response is too low in this case. From the top-bottom measurements (lower Fig. 7), two absorption thresholds are extracted from Tauc plots. The direct absorption threshold is also obtained at 2.73 eV while the indirect bandgap is extracted at 2.25 eV (insert curve Fig. 7). Both values are consistent with the expected value of GaP bandgaps (2.26 eV for the indirect bandgap and 2.78 eV for the direct bandgap at 300 K) [14]. One notice that there is no additional signal in the EQE measurements after 520 nm. Therefore, there is no signal arising from the silicon substrate.

Finally, the values of the short-circuit electrical currents have been extracted from the EQE. It gives 2.1 mA/cm^2 for the top-top sample. The calculated value of J_{SC} from the EQE is larger than the measured one with the L-I-V measurement (0.8 mA/cm^2 for the top-top, as shown in the following). When the J_{SC} is lower than EQE, this can be attributed to a barrier for the photo current. A small current density of a EQE measurement can pass the barrier while a high current density under AM1.5 illumination cannot overcome the barrier. This difference is also linked to the top-top solar cell geometry. To calculate J_{SC} from I-V measurement, the short circuit intensity is divided by the solar cell surface of $365 \times 290\,\mu m^2$, assuming that the intensity is evenly distributed over the entire surface of the mesa, including the part hidden by the metallic contact. On the contrary, one can assume that carriers are mostly generated under the illuminated area and collected by the contact edge. With this hypothesis, J_{SC} reaches 2.3 mA/cm^2, on the same order of magnitude as J_{SC} extracted from EQE. Concerning the top-bottom cell, the short-circuit electrical current has been extracted from the EQE, giving 1.2 mA/cm^2. The calculated value of J_{SC} from the EQE is almost the same as compared with the

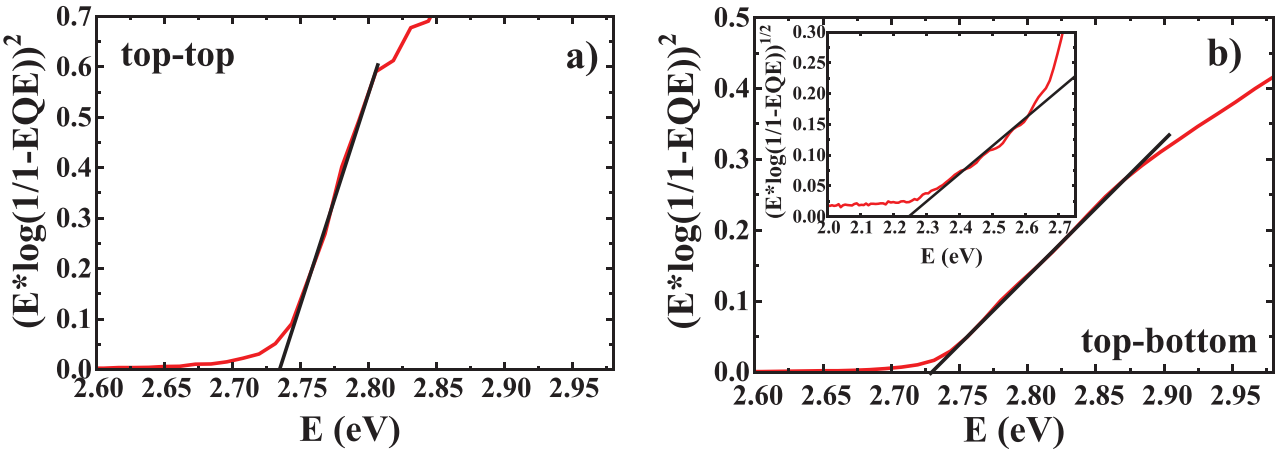

Fig. 7. EQE Tauc plots of the direct transition for (a) both the top-top electrical contacts configuration and (b) the top-bottom electrical contacts configuration (insert: EQE Tauc plot for the indirect transition).

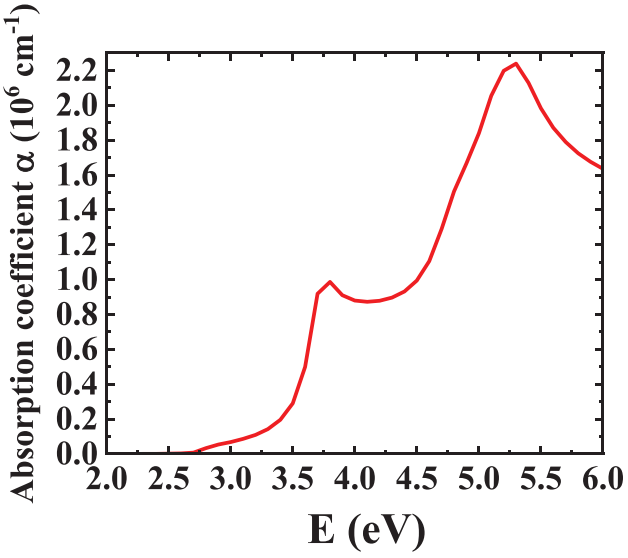

Fig. 8. Absorption coefficient of crystalline GaP, from Ref. [15].

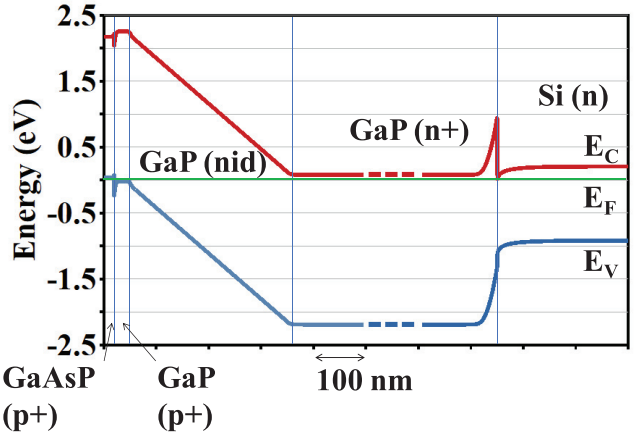

Fig. 9. Simulated band diagram of the solar cell, in dark at zero voltage.

measured one from the L-I-V curve (1.5 mA/cm^2 for the top-bottom). The small discrepancy between both values is too low to be relevant since it may be due to different experiment conditions.

According to the absorption coefficient value shown on Figure 8 [15], and considering a simple Beer-Lambert absorption law, giving a rough approximation, around 91% of the incoming flux is absorbed in 350 nm of GaP at 3 eV, and 99% at 3.3 eV (and not taking into account the 1 µm-thick *n*-type and *i*-type GaP layers below the GaP absorber, in a first approximation). Considering also the transmission coefficient of GaAsP at 3 eV (62.4%) and at 3.3 eV (60.7%) [15], one can consider, in a rough approximation and according to the fact that our solar cell does not contain any anti-reflection coating (ARC), that the maximum theoretical external quantum efficiency (EQE) is equal to 57% at 3 eV, and 60% at 3.3 eV.

We can remark that the EQE was between 55% and 60% at 3 eV and between 45% and 65% at 3.3 eV, close to the maximum theoretical EQE values, which means that the absorption properties of this GaP solar cell is very good. Moreover, the carrier's extraction is also very good at these small current densities.

Considering the top-bottom one, the overall EQE is lower than in the top-top configuration due to some difficulties to extract the carriers, since the absorption properties of the two solar cells configurations should be similar (the absorption thickness being the same). Therefore, the defects at the GaP/Si interface (limited diffusion lengths in the different materials, losses at the electrical contacts, etc...). or a barrier at the GaP/Si interface seem to decrease the solar cell performances. Figure 9 shows the simulated band diagram of the solar cell, only taking into account the doping levels and the conduction band offsets proposed by Ref. [16], at equilibrium. GaP/Si interface presents a theoretical conduction band offset of 0.92 eV, inducing a triangular barrier extended on almost 25 nm at the GaP/Si interface.

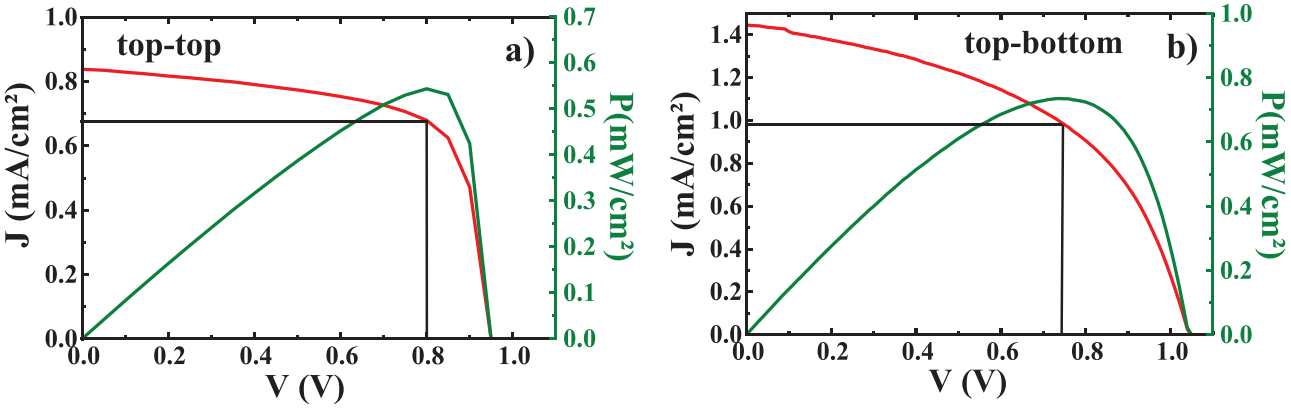

Fig. 10. L-I-V curve from a solar simulator, in conventional solar cell operation, on (a) the "top-top" configuration solar cell and (b) the "top-bottom" one. The green curves are the P-V curves obtained with the L-I-V.

Table 1. Electrical characteristics of top-top and top-bottom cells.

	V_{OC} (V)	J_{SC} (mA/cm^2)	V_{max} (V)	J_{max} (mA/cm^2)	FF	η	$\eta_{theoretical}$
Top top	0.95	0.837	0.80	0.680	0.68	0.57%	8%
Top bottom	1.043	1.493	0.74	1.004	0.48	0.77%	8%

Some improvements are possible to overcome the carriers' extraction limitation, for instance by decreasing the GaP thickness below the absorber, which was fixed at 1 µm in a first step, in order to ensure a sufficient good crystallinity of the GaP absorber. An optimization of the growth of doped GaP directly onto the *n*-doped silicon substrate would allow to dramatically decrease the buffer thickness and would allow to decrease the interface defects density [8], therefore improving the carriers harvesting. To reduce the barrier extend, doping level in GaP (n) has to be increased to enhance tunnelling.

3.2 I-V characteristics

The I-V curve under solar light illumination for both cells are shown in Figure 10, which also shows the P-V curve in order to measure the bias at the maximum electrical power. Table 1 summarizes the electrical performances of the two types of cells.

The top top solar cell (Fig. 10a) presents a window to harvest the solar light much smaller than the mesa surface. Therefore, we propose a corrected conversion efficiency in this case, taking into account the ratio of the cell window surface of 39.10^{-5}cm^2 and the mesa surface of 106.10^{-5}cm^2. Considering this ratio, the corrected conversion efficiency reaches 1.48%.

Considering the direct energy bandgap of GaP (2.7 eV), the theoretical maximum light to power conversion efficiency (detailed balance limit) for a solar cell operating at 298 K and illuminated with the AM 1.5G spectrum is arround 8% [17,18]. The corrected conversion efficiency obtained in this work (1.48%) is around 18.5% of the theoretical value calculated from the Shockley-Queisser limits. This result is therefore encouraging for our work.

For the top-bottom cells, no correction is needed to take into account the window surfaces the efficiency only reaches 0.77%. Considering the large GaP bandgap, this value is around 10% of the theoretical value.

Figure 11 shows the superimposed I-V curves in the dark and under solar light illumination, in a logarithmic scale for both cells. One can remark that the D-I-V curve shows a hysteresis around 1.4 V − 1.5 V for the top-bottom cell (Fig. 11b) while this hysteresis appears for both light and dark I-V curves for the top-top cell between 1.3 and 1.7 V (Fig. 11a). For both cells, this hysteresis appears at a larger voltage than the solar cell regime. At such a high voltage, some carriers may reach the GaP/Si interface even in the case of top-top cells. A potential barrier at the GaP/Si interface can be the cause of this hysteresis which needs further investigation.

To examine better the solar cells properties, the R_s and R_{sh} resistances have been determined, in a first approximation, through the slope of the I-V curve between −0.5 V and 0 V for R_{sh} and between 1 mA/cm^2 and 1.5 mA/cm^2 for R_s. Table 2 summarizes the resistances values for both cells. Let us notice that these values are less accurate than values from a simulation but can be used as factor-of-merit to compare different samples. Therefore, the illumination yields to the increase of shunting paths inside the p-n diode. This can be due to some threading defects inside the stacking (dislocations due to the relaxation of the lattice mismatch, antiphase domains). However, the series resistance seems to be lower in the L-I-V measurement than in the D-I-V one.

For the top bottom case, all the resistances are around one order of magnitude larger than in the top-top case, which explains the lower FF value and therefore the lower efficiency, despite a larger J_{SC} in the top-bottom case.

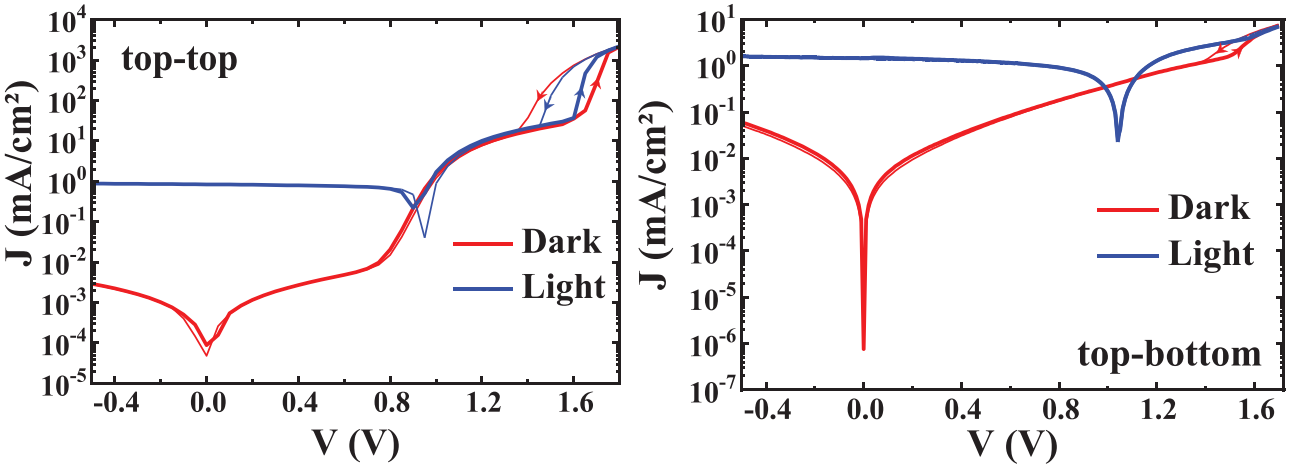

Fig. 11. L-I-V and D-I-V curves in a logarithmic scale and in large scale for (a) top-top contacts, and (b) top-bottom contacts.

Table 2. Comparison of the estimated values of shunt and series resistances for both cells.

	D-I-V R_s (Ω.cm^2)	L-I-V R_s (Ω.cm^2)	D-I-V R_{sh} (Ω.cm^2)	L-I-V R_{sh} (Ω.cm^2)
Top top	53	34	1.8×10^5	1.1×10^4
Top bottom	308	120	1.0×10^4	3.33×10^3

A comparison between the top-top and the top-bottom configurations seems to indicate that the passage through the GaP/Si interface probably degrades a little bit the characteristics of the solar cells in terms of fill factor (due to the degradation of both the series resistance and the shunt resistance). Indeed, top-top contacts sample has a fill factor (FF) of 0.68, which is better than top-bottom contacts sample of 0.48. A first explanation is the fact that top-top contacts sample has a lower series resistance as revealed by the L-I-V shape. A larger series resistance is probably due to the remaining structural defects at GaP/Si interface and the barrier potential for electrons at this interface. These two effects also can explain the lowering of EQE. However, the results obtained on the top-bottom configuration are sufficiently interesting to develop the III-V/Si tandem cells in the future.

4 Conclusions

A GaP n-i-p photodiode grown on silicon substrate has been studied. It could serve as a top cell in the tandem cell structure onto silicon substrate. For both top-top and top-bottom electrical contacts, we obtain efficiencies equal to 1.48% and 0.77% respectively, which reach almost 18.5% of the theoretical efficiency value set by Shockley-Queisser limits. This top cell structure is suitable for the development of tandem cell onto silicon and any other III-V photonic devices onto silicon too. This experimental study of the effect of the GaP/Si interface for solar cells paves the way towards the development of GaP based tandem cells.

The authors thank Laurent Le Brizoual for his expertise on solar simulator experiments. F. Fan thanks the Chinese Scholarship Council for funding. The authors acknowledge RENATECH+ (French Network of Major Technology Centers) for technological support and the Région Bretagne support.

Author contribution statement

Sample growth and structural characterization were conducted by T. Rohel, R. Bernard, A. Létoublon and C. Cornet. Technological steps were conducted by K. Tavernier and C. Levallois. Solar cell experiments were conducted by F. Fan, A. Beck and S. Boyer-Richard. The supervision of the project was ensured by O. Durand. The writing of the manuscript was performed by S. Boyer-Richard and O. Durand and proof reading by all co-authors.

References

1. S. Almosni et al., Correlations between electrical and optical properties in lattice-matched GaAsPN/GaP solar cells, Sol. Energy Mater. Sol. Cells **147**, 53 (2016)
2. K. Yamane, K. Sato, H. Sekiguchi, H. Okada, A. Wakahara, Doping control of GaAsPN alloys by molecular beam epitaxy for monolithic III-V/Si tandem solar cells, J. Cryst. Growth **473**, 55 (2017)
3. S.P. Bremner, M.Y. Levy, C.B. Honsberg, Analysis of tandem solar cell efficiencies under AM1.5G spectrum using a rapid flux calculation method, Prog. Photovoltaics Res. Appl. **16**, 225 (2008)

4. NREL, *Best research-cell efficiency chart*, https://www.nrel.gov/pv/cell-efficiency.html
5. M. Da Silva et al., GaAsPN-based PIN solar cells MBE-grown on GaP substrates: toward the III-V/Si tandem solar cell, in *Physics, Simulation, and Photonic Engineering of Photovoltaic Devices IV*, **9358**, 93580H (2015)
6. N. Jain, M.K. Hudait, III–V multijunction solar cell integration with silicon: present status, challenges and future outlook, Energy Harvest. Syst. **1**, 121 (2014)
7. S. Almosni et al., Evaluation of InGaPN and GaAsPN materials lattice-matched to Si for multi-junction solar cells, J. Appl. Phys. **113**, 12 (2013)
8. Y. Ping Wang et al., Abrupt GaP/Si hetero-interface using bistepped Si buffer, Appl. Phys. Lett. **107**, 191603 (2015)
9. T. Soga, T. Jimbo, M. Umeno, Dislocation generation mechanisms for GaP on Si grown by metalorganic chemical vapor deposition, Appl. Phys. Lett. **63**, 2543 (1993)
10. Y. Ping Wang et al., Quantitative evaluation of micro twins and antiphase defects in GaP/Si nanolayers for a III–V photonics platform on silicon using a laboratory X-ray diffraction setup, J. Appl. Crystallogr. **48**, 702 (2015)
11. A. Katz, B.E. Weir, W.C. Dautremont-Smith, Au/Pt/Ti contacts to p -In 0.53 Ga 0.47 As and n -InP layers formed by a single metallization common step and rapid thermal processing, J. Appl. Phys. **68**, 1123 (1990)
12. C. McDonald et al., Zero-dimensional methylammonium iodo bismuthate solar cells and synergistic interactions with silicon nanocrystals, Nanoscale **9**, 18759 (2017)
13. B.G. Mendis et al., Nanometre-scale optical property fluctuations in Cu2ZnSnS4 revealed by low temperature cathodoluminescence, Sol. Energy Mater. Sol. Cells **174**, 65 (2018)
14. I. Vurgaftman, J.R. Meyer, L.R. Ram-Mohan, Band parameters for III–V compound semiconductors and their alloys, J. Appl. Phys. **89**, 5815 (2001)
15. D.E. Aspnes, A.A. Studna, Dielectric functions and optical parameters of Si, Ge, GaP, GaAs, GaSb, InP, InAs, and InSb from 1.5 to 6.0 eV, Phys. Rev. B **27**, 985 (1983)
16. C.G. Van de Walle, J. Neugebauer, Universal alignment of hydrogen levels in semiconductors, insulators and solutions, Nature **423**, 626 (2003)
17. W. Shockley, H.J. Queisser, Detailed Balance Limit of Efficiency of p-n Junction Solar Cells, J. Appl. Phys. **32**, 510 (1961)
18. S. Rühle, Tabulated values of the Shockley–Queisser limit for single junction solar cells, Sol. Energy **130**, 139 (2016)

Cite this article as: Soline Boyer-Richard, Fei Fan, Alexandre Beck, Christophe Levallois, Karine Tavernier, Tony Rohel, Rozenn Bernard, Antoine Létoublon, Charles Cornet, Olivier Durand, Investigation of III-V GaP solar cell on silicon substrate, EPJ Photovoltaics 14, 31 (2023)